Fatigue of bridge joints using welded tubes or cast steel node solutions

A. Nussbaumer & S. C. Haldimann-Sturm
Swiss Federal Institute of Technology Lausanne (EPFL), ICOM – Steel structures Laboratory, Switzerland

A. Schumacher
Swiss Federal Laboratories for Materials Testing and Research (EMPA), Structural Engineering Research Laboratory, Dübendorf, Switzerland

ABSTRACT: In the design of recently constructed steel-concrete composite bridges using hollow section trusses for the main load carrying structure, the fatigue verification of the tubular truss joints has been a main issue. Recent research on the fatigue behaviour of such joints has focussed on circular hollow section (CHS) K-joints with low diameter-to-thickness ratios—a geometric characteristic typical to tubular bridge trusses. Analytical and experimental research was carried out and joints with both directly welded tubes and cast steel nodes were studied. This paper presents the main results of these studies and shows comparisons between welded and cast steel solutions. The key issues for the design and fabrication of both types of nodes are reviewed and recommendations for the design and fabrication of tubular bridge structures are made.

1 INTRODUCTION

Tubular joints represent the critical point in the design of a bridge structure with circular hollow section (CHS) members. Presently, three main methods of joint fabrication can be found in existing bridges. A conventional possibility consists of brace-to-chord connections using gusset plates. This solution will not be dealt with in this paper. The second possibility is the directly welded joint, where the braces are cut to fit and welded to the continuous chord. Cast steel nodes offer a third alternative whereby castings are employed to provide a smooth transition between the brace and chord members, which are welded to the casting stubs.

The second and third mentioned solutions have been extensively studied by the offshore industry (Marschall 1992). However, the relatively new concept of steel-concrete composite CHS truss bridges presents the designer with new challenges, in particular with respect to the fatigue design of the joints. In comparison to offshore structures, differences in member sizes, tube slenderness, fabrication techniques, etc. make the direct application of the current offshore knowledge difficult and demonstrate that the current behaviour models for welded joints and cast nodes subjected to fatigue are incomplete.

For the designer, an important question is whether to choose welded joints or cast nodes in order to insure better fatigue strength for a given project. The lack of existing fatigue design rules has been the underlying motivator for a series of studies on the fatigue behaviour of directly welded joints and of cast steel nodes in tubular truss bridges carried out at the Steel Structures Laboratory (ICOM-EPFL) in Lausanne, Switzerland. The experimental studies are fully described by Schumacher (Schumacher 2003a, Schumacher & Nussbaumer 2006) and Haldimann-Sturm (Sturm et al. 2003 and Haldimann-Sturm 2005). In this paper, the comparison between both solutions is discussed. In the case of welded CHS K-joints, the determination of the stress concentration factors (SCF), synthesised in the form of a modified stress concentration factor (referred to as SCF_{total}.), is explained. In the case of cast steel nodes, the importance of a balanced design between the various potential crack initiation sites in a joint is shown.

2 EXPERIMENTAL STUDIES

2.1 *General*

In order to include all aspects influencing the fatigue strength, fatigue tests on large-scale specimens have been carried out. The specimens consisted of K-joints in a planar truss girder (Figure 1). The material used for the truss members was steel grade S 355J2H according to EN 10210-1:1994 and EN 10210-5:1997. The material used for the castings was steel grade GS20Mn5V according to EN 17182. Regarding the allowable casting defects, the quality of the castings was defined according to DIN 1690,

Part 2. The test specimen (shaded in Figure 1) was bolted in place by means of end plates. The top chord I-girder and the two outer K-joints acted as a load frame to the two inner K-joints. Both the welded joints and cast nodes were tested in the same way. For comparison purposes, Figure 1 shows half of a truss girder with welded joints (on the left side) and the other half with cast steel nodes (on the right side). The constant amplitude fatigue loading, with a load ratio of 0.1, was applied at midspan through hydraulic actuators. Joint failure was defined as through-cracking of the tube or cast node wall.

For the directly welded joints, Schumacher (Schumacher 2003a) carried out a total of 4 test series with 2 test specimens per series. Each test series examines a particular parameter: dimension, fabrication method or weld improvement. The non-dimensional parameters (β, γ, τ, θ, defined in Figure 1) of the specimens were chosen to reflect actual CHS truss bridge parameters. Except for the weld-improved specimens, twelve out of the sixteen welded joints cracked at the same location and in the same manner. Cracks initiated in the chord gap region at the tension brace weld toe, referred to as Location 1 (Figure 2). This corresponded with the location of the highest measured hot-spot stress. Crack propagation occurred through the depth of the chord as well as along the weld toe.

For the cast steel nodes, two series (A and B) with 2 resp. 3 test specimens per series were carried out. The tests were carried out to investigate the fatigue strength of the cast steel nodes as well as the fatigue strength of the girth butt welds between the CHS members and the casting stubs. Several parameters were studied: cast steel quality, weld type at stub connections and stiffness parameters. The last parameter includes changes in the CHS thickness, thickness ratios and stub length. This serves the purpose of studying the influence of the stiffness difference between cast steel nodes and CHS members on the global behaviour as well as on the stress distribution near the butt welds and in the cast steel nodes. Except for two specimens of series B, where no cracking occurred and testing was stopped after a certain number of cycles, all cracks initiated in the girth butt welds between the casting stubs and the CHS members with the highest measured stress (Figure 2). That is, no fatigue cracking due to casting defects were detected in the cast steel nodes. In additional destructive and non-destructive testing on cast steel nodes, no non-allowable casting defects, which could have been an initiation site of fatigue cracking, could be found. It could be concluded that in these tests, the girth butt welds were much more susceptible to fatigue loading.

2.2 *Comparison of results*

Since tests on girders with welded joints and cast steel nodes were carried out on a truss girder with similar geometry and loading, it is interesting to compare the results. When mentioning the test results of cast steel nodes, it is the test results of the girth butt welds of the cast nodes to which reference is being made, since no fatigue cracking was observed in the nodes themselves. In other words, the fatigue strength of the girders with cast nodes was, in fact, determined by the fatigue strength of the girth butt welds.

The comparison is mad e on the basis of hot spot stress range values $\Delta\sigma_{R,hs}$. Therefore, the hot spot stresses in the girth butt welds of the cast steel nodes are obtained by multiplying the nominal stresses in the chord with a stress concentration factor according to DNV recommendations (DNV 2001) to take into account the eccentricity in the weld due to differences in thickness and diameter. The hot spot stresses in the directly welded joints were extrapolated from the strain measurements near the weld toe of the tension brace.

In Figure 2, test results of series S1 and S2 (with identical chord thickness) for the directly welded nodes are represented by the black rhombi. The corresponding characteristic *S-N* curve was found based on IIW rules. The triangular points show the test results for the girth butt welds without and with back-

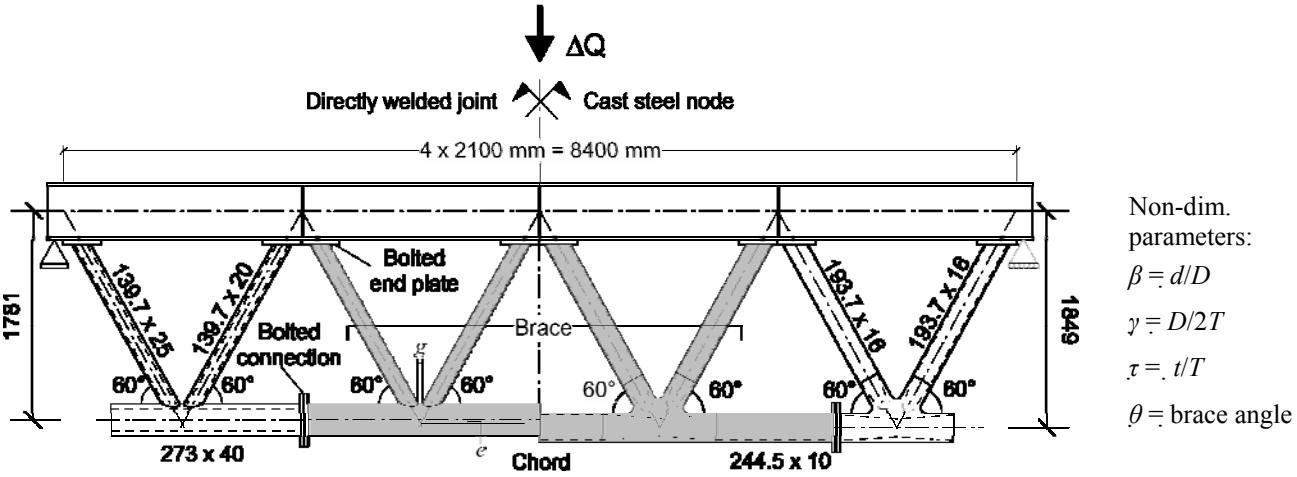

Figure 1. Test specimen, only half represented with directly welded joints (left) and cast steel nodes (right).

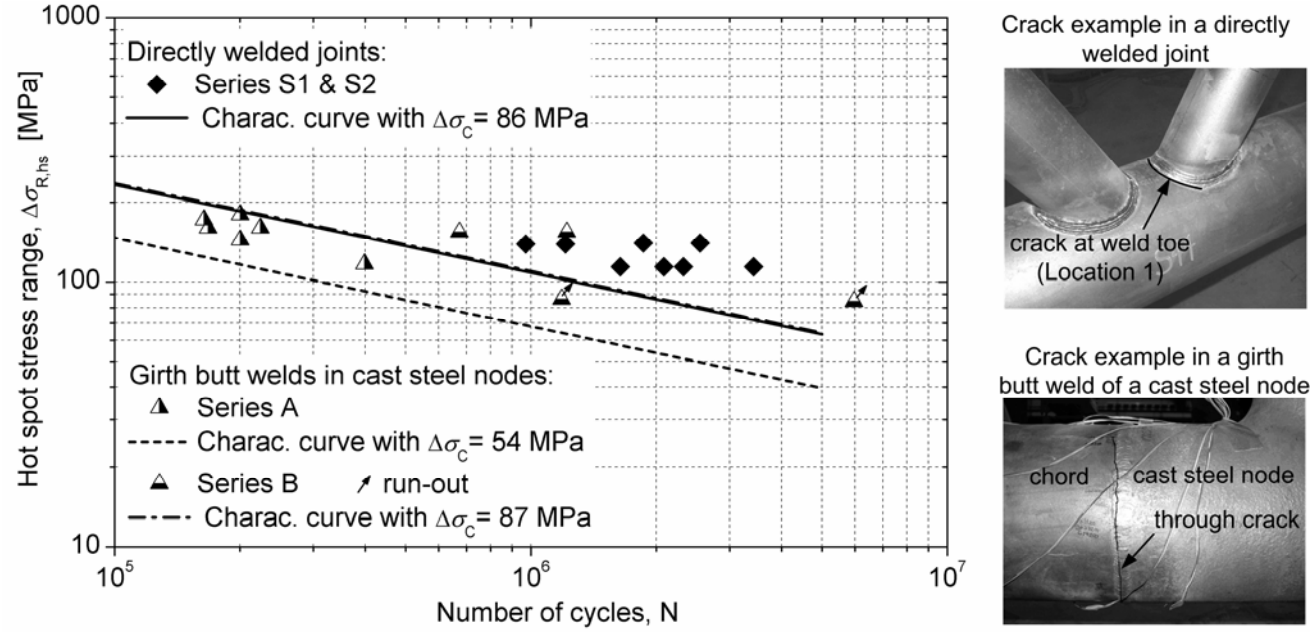

Figure 2. Hot-spot *S-N* results for tests on welded joints and cast nodes (girth butt welds)

ing bars (series A and B, resp.). The corresponding characteristic *S-N* curve has been established by subtracting two standard deviations of log(*N*) from the mean curve. A standard deviation of 0.2 typical for welded girders was used because only few test results are available to represent a significant sample of test data. It can be seen that the results for the welded joints come to a fatigue strength at $2 \cdot 10^6$ cycles of $\Delta\sigma_C = 86$ MPa which is similar to $\Delta\sigma_C = 87$ MPa for the girth butt welds with backing bars. There is, however, a significant difference in the fatigue behavior between the two types of tests: in the welded joints, cracking is directed by high stress concentrations at the weld toes and in the cast steel node joints cracking is caused by weld root defects in the girth butt welds at the casting stubs. Furthermore, the fatigue strength of $\Delta\sigma_C = 54$ MPa of the girth butt welds *without* backing bars is much lower. More testing on girth butt welds between casting stubs and CHS members is currently being carried out by the Versuchsanstalt für Stahl, Holz und Steine at the Technische Universität Karlsruhe, Germany.

As shown in Figure 2, the fat. strength of the welded joints at $2 \cdot 10^6$ cycles is 86 MPa. In comparison, is it known from literature that the fat. strength at $2 \cdot 10^6$ cycles of the cast steel nodes alone lies between 100 and 165 MPa (Haldimann-Sturm 2005), depending mainly upon casting quality. Although the strength of the cast nodes is considerably higher than the welded joints, this was found to be irrelevant in the present tests, since this higher capacity could not be mobilized as failure was governed by the connections between the casting stubs and the CHS members. In the present study, any type of comparison (nominal stress, hot-spot, etc.), if properly done, shows that both solutions have about the same fatigue strength. As discussed in Section 3.2, it is possible to find an optimum in the design by relaxing the quality requirements on the cast nodes, thus reducing their cost. This way, a balanced and economical design between the various potential crack initiation sites in a joint is obtained.

2.3 *Pros and cons*

The root cracking of the girth butt welds for cast steel nodes can be seen as a disadvantage in comparison to the directly welded joints. Two main reasons can be given. First, it is impossible to perform non destructive testing (NDT) or to apply a post weld treatment to the girth butt welds, because the root is generally not accessible. During a bridge inspection, only through-thickness cracks can be visually detected. Second, there are at least four such welds in each node (in the case of a K node). They are the most critical detail and diminish the fatigue strength of the whole structure if not properly designed.

Looking at a truss girder with cast nodes, two girth butt welds are necessary at each node in the chord to ensure continuity, which means that weld quality must be of a high and constant level to guarantee fatigue reliability. Also, with the high number of girth butt welds, pre-assembly and assembly sequences must be well studied in order to properly manage weld shrinkage and to respect tolerances. The advantage is that all weld preparations are simple, on straight edges and with constant bevel angle. This is, however, not the case for on-site assembly. The last tube cannot be placed in the assembled truss if the backing rings, necessary to ensure good weld quality, are already welded. This problem can be solved by adding cut-outs. In this way, the backing rings are movable during the assembly of the tube. Once the tube is put in place, the backing rings are pushed to the right position for welding. An example of these

movable backing rings is shown on Figure 3 (Raoul 2005).

Figure 3. Movable backing ring for on-site assembly

In the case of welded truss girders, the chord continuity is an advantage, especially for the tension chord, when speaking about fatigue reliability. There are no girth butt welds except at CHS section changes, at assembly joints between two tube members and at site joints. However, this advantage disappears partially for large bridges with spans over 80 m, since the maximum deliverable tube length (for diameters over 500 mm and thicknesses over 25 mm) is less than 10 m. In these cases, the number of butt welds will approach the one of the cast steel node solution.

There are, on the other hand, also several advantages of cast nodes, for example, their ability to manage any geometry and number of incoming members. For welded joints, there are limitations due to minimum required angles between incoming CHS members, gaps and eccentricities. Also, the smooth geometry of cast nodes leads to low SCFs and it is possible to integrate special features such as parts of bearings or connectors to the concrete deck directly into the castings. As a result, cast nodes are particularly suited for nodes near or at supports, where the bending moment is negative and where there are usually more incoming tubes at the nodes.

3 NUMERICAL STUDIES AND DESIGN METHODS

3.1 *Tubular welded joints*

The concept of the hot spot stress (Marshall 1992, Zhao et al. 2000 and Zhao & Packer 2000b) was used in the interpretation of test results. It has been proven to be the best solution to properly account for the complexity in the stress distribution in tubular joints and to quantify the observed fatigue behavior. Moreover, hot spot stress values can also be determined by FEM calculations using a validated standard procedure as explained in Schumacher (2003a). The software programs I-DEAS® and ABAQUS® were used to develop FE models of the truss girder and of the K-joints. The welds were also included in the models.

A large parametric study with over 200 FE models was performed on a range of welded joints to examine the effects of geometry and load. In particular, the study of low γ, between 4 and 12, values typical to bridges, differentiates the present parametric study from previous, comparable studies. The study led to the proposal of SCFs (Schumacher 2003a) for ranges of non-dimensional parameters (β, γ, τ, θ) not yet available. Furthermore, the intuitive fatigue design method summarized below was proposed.

The concept of the hot spot stress gives the total hot spot stress $\sigma_{\mathrm{hs},i}$, at a joint Location i in the node, due to a combination of nominal member stresses (both in the brace *and* the chord). It is usually expressed as the summation of the contribution from each individual load case (noted LC):

$$\sigma_{\mathrm{hs},i} = \sum_{LC=1}^{n} \sigma_{LC} \cdot SCF_{i,LC} \tag{1}$$

Where n is the total number of individual load cases necessary to represent a real load condition. This equation can be rearranged by expressing the percentage of each stress component, for example $\sigma_{\mathrm{ax\_br}}$, as a percentage $P_{\mathrm{ax\_br}}$ of the total nominal stress σ_{total}. In a more general way, this results in the following:

$$\sigma_{\mathrm{hs},i} = \sigma_{\mathrm{total}} \cdot \sum_{LC=1}^{n} \frac{P_{LC}}{100} \cdot SCF_{i,LC} = \sigma_{\mathrm{total}} \cdot SCF_{\mathrm{total},i} \tag{2}$$

$\sigma_{\mathrm{hs},i}$ hot spot stress at joint Location i

σ_{total} total nominal stress affecting the joint, $\sigma_{\mathrm{total}} = \sigma_{\mathrm{nom\_ch}} + \sigma_{\mathrm{nom\_br}}$ The nominal stresses in chord $\sigma_{\mathrm{nom\_ch}}$ resp. in brace $\sigma_{\mathrm{nom\_br}}$ correspond to the superposition of axial and bending stresses.

P_{LC} percentage of member stress, due to load case LC, with respect to total stress

$SCF_{i,LC}$ stress concentration factor at joint Location i, for load case LC

$SCF_{\mathrm{total},i}$ total stress concentration factor at joint Location i

The total stress concentration factor can be represented as shown in Figure 4, for given geometry parameters and a given stress partition in the members. A given ratio of stresses due to axial load and in-plane bending in the brace and chord member was assumed as recommended in current design guidelines (Zhao 2000b).

The total stress concentration factor is given as a function of the percentage of member stresses, which are expressed as the brace stress ratio:

$$\frac{\sigma_{\text{nom\_br}}}{\sigma_{\text{total}}} = \frac{\sigma_{\text{nom\_br}}}{\sigma_{\text{nom\_br}} + \sigma_{\text{nom\_ch}}} \quad (3)$$

$\sigma_{\text{nom\_br}}$ total nominal stress in the tension brace
$\sigma_{\text{nom\_ch}}$ total nominal stress in the chord.

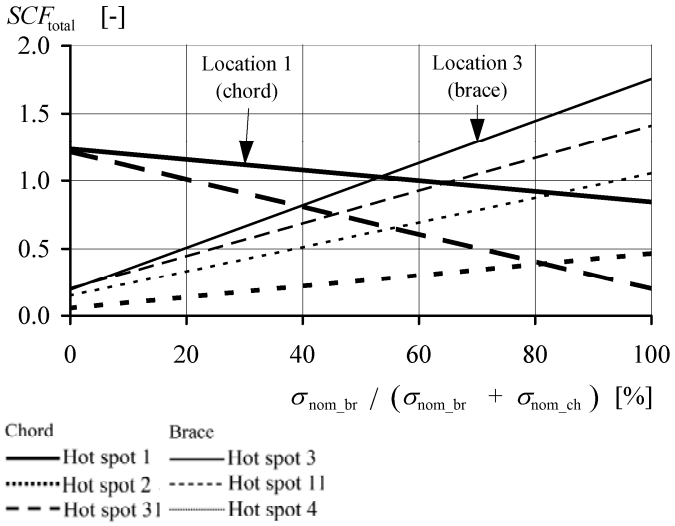

Figure 4. SCF_{total} calculated for non-dimensional parameters $\beta = 0.5$, $\gamma = 4$, $\tau = 0.3$ and $\theta = 60°$

The advantages of this representation are that all potential crack locations can be plotted on one graph. For design, only the envelope can be given (Locations 1 and 3 in Figure 4), since these locations govern. Note that the denominator in Equation (3) implies a scalar superposition of member stresses; the fact that the stresses act in different directions is accounted for by individual SCFs. For usual stress partition values, the designer has at his disposal a set of graphs from which can be extracted the proper SCF_{total}.

Table 1. Parameter values and stress partitions covered

				Stress partition in members [%]	
θ	β	γ	τ	**Brace**	**Chord**
[°]	[-]	[-]	[-]	$\Delta\sigma_{ax} / \Delta\sigma_{bend}$	$\Delta\sigma_{ax} / \Delta\sigma_{bend}$
45	0.50 – 0.70	4.0 – 30.0	0.30 – 0.70	75/25	65/35
60	0.50 – 0.70	4.0 – 30.0	0.30 – 0.70	75/25	65/35
45	0.50 – 0.70	4.0 – 30.0	0.30 – 0.70	100/0	100/0
60	0.50 – 0.70	4.0 – 30.0	0.30 – 0.70	100/0	100/0
45	0.50 – 0.70	4.0 – 30.0	0.30 – 0.70	0/100	0/100
60	0.50 – 0.70	4.0 – 30.0	0.30 – 0.70	0/100	0/100

Table 1 summarizes the range of parameters for the set of graphs that were developed for practical applications (Schumacher 2003b). From Figure 4, it can also be seen that the SCF_{total} always stays below a value of two. This figure does not show an isolated result; relatively low SCF values were found throughout the study. It was concluded that there is a strong tendency for SCF values to decrease with decreasing γ values. A low γ value, inferior to seven as seen with existing bridges, is therefore a desirable geometric characteristic. This should be reflected more in design specifications, which currently fix a recommended minimum stress concentration factor of $SCF = 2.0$, a value very penalizing if applied to bridges with low γ values. For bridge applications, the minimum value can be taken as $SCF = 1.0$. However, one reason for a recommended minimum value of 2.0 comes from the concern of possible root cracking if too low values are used for weld toe fatigue design. If the recommended minimum SCF is lowered, it must be done in conjunction with the requirement of full penetration for all welds in CHS joints.

3.2 *Cast steel nodes with girth butt welds*

The fatigue test results have shown that cast nodes have a far better fatigue strength, but that this capacity cannot be mobilized as failure is governed by the connections between the casting stubs and the CHS members. A numerical study has been carried out to quantify allowable initial sizes of defects in cast nodes in order to provide a balanced design between the various potential crack initiation sites, especially between the girth butt welds and the cast steel node.

To find the internal forces under fatigue and ultimate load acting on a cast steel node in a tubular bridge structure, a typical steel-concrete composite bridge was defined based on the properties of existing tubular bridge structures described in Sturm et al. (2003) and Velselcic et al. (2003). The study is limited to the two most critical nodes at different locations along the bridge with varying internal load configurations acting on the casting stubs. At midspan, the axial brace forces are much lower than in a node near an intermediate support. For this truss configuration, a cast node shape with minimal stub length has been chosen because secondary bending moments acting at the casting stub ends reach their maximum for this case.

The software BEASY® was used to develop a boundary element (BE) model of the cast steel node to simulate propagation of cracks initiating from a casting defect (Figure 5). Due to the longitudinal symmetry, only half of the cast steel node was modelled. The out-of-plane displacements were constrained in the plane of symmetry (not shown in Figure 5). The casting defects at different locations i in the node were modelled as two-dimensional cracks, representing all types of casting defects. This is a very conservative assumption as the fatigue behaviour of a two-dimensional crack is much more critical than that of casting defects like gas holes, slack inclusion or shrinkages. Figure 5 shows the 9 different locations in the cast nodes where the allowable initial sizes $a_{0,i}$ of casting defects are quantified. At

Location 7, an inner crack has been assumed; at all other locations, more critical surface cracks were introduced in the cast node model.

The difference of the stress intensity factor $\Delta K(a)$ is needed for crack propagation calculations. When moving the fatigue load (for this bridge example according to the Swiss design code, SIA 261 (2003)) across the bridge, it is not obvious which load position induces the minimum and the maximum stress intensity factor (SIF) at a defect in the node. For this reason, the SIF influence lines of an identical crack at the 9 locations in the node were calculated considering the internal forces which are induced by the moving fatigue load. Knowing the influence line of the SIF and the crack propagation plane, the two load positions defining $\Delta K_I(a)$ for mode I could be determined.

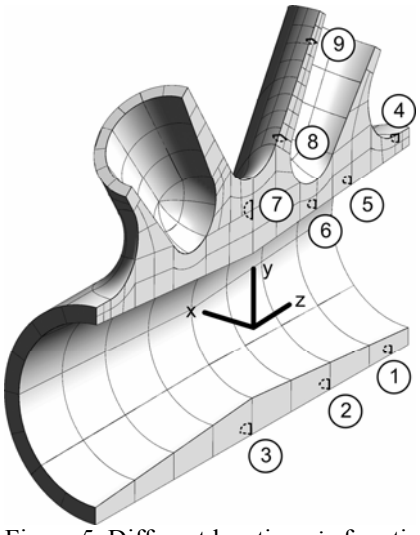

Figure 5. Different locations *i* of casting defects

Under fatigue loading, crack propagation at Location *i* of the node was simulated using the software BEASY®. The results are given at intermediate steps in terms of crack configuration, crack depth a and the appropriate maximum and minimum stress intensity factors $K_{I,max}$ and $K_{I,min}$ (Figure 6 shows $K_{I,max}$). The final crack depth a_f was limited to a minimum of 90 % of the wall thickness and the critical crack size in the case of brittle fracture, which was found using the failure assessment diagram (FAD) (Milne 1986). For this purpose, the stress intensity factor under ultimate static loading $K_{I,ULS}$ was needed. The results showed that brittle failure of a node containing cracks does not occur. A crack depth equal to 90 % of the wall thickness at the crack location was therefore chosen as the failure criterion, assuming that a through-thickness crack is unacceptable.

Once the final crack size a_f was known, the initial allowable crack size a_0 could be back-calculated using the Paris-Erdogan equation. As the BEASY® output for crack propagation simulations consists of discrete stress intensity factor values (Figure 6), the Paris-Erdogan equation can only be solved discretely:

$$N_{tot} = \sum_{k=0}^{n-1} \Delta N_k = \frac{1}{C} \cdot \left[\frac{a_1 - a_0}{\Delta K_{I,0}^m} + \frac{a_2 - a_1}{\Delta K_{I,1}^m} + \ldots + \frac{a_n - a_{n-1}}{\Delta K_{I,n}^m} \right] \quad (4)$$

N_{tot} service life in terms of the number of loading cycles

C crack propagation parameter, $C = 2 \cdot 10^{-13}$ (mm / cycle)·(N·mm$^{-3/2}$)$^{-m}$

m crack propagation parameter, $m = 3$

a_n final crack size a_f

According to (Blair 1995) the crack propagation parameters for cast steel correspond to those of ferritic-perlitic steel. For the back-calculation, the following assumptions were made:

- A service life of 70 years according to (SIA 261 2003); the fatigue loads were adapted to correspond to a service life of $2 \cdot 10^6$ cycles.
- The cracks behaved as long cracks (and not as short cracks) and with no initiation period.
- Deterministic calculations were carried out.
- For the brittle failure verification, the fracture toughness under quasi-static loading was used.

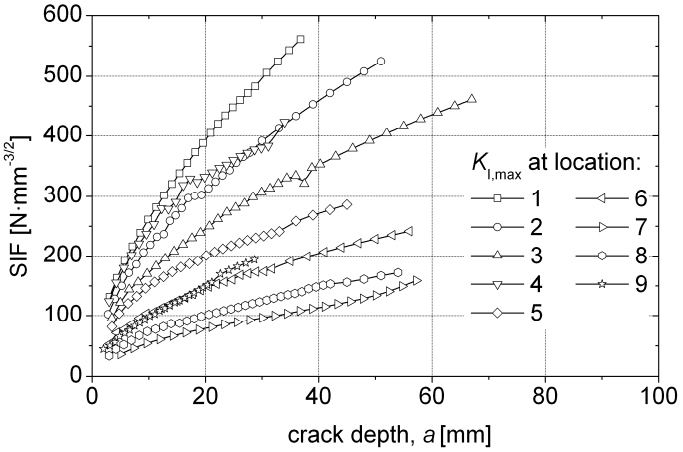

Figure 6. Examples of SIF results at different crack locations in the node at midspan

The resulting allowable initial defect sizes for the typical steel-concrete composite bridge are very large. They vary between approximately 28 and 88 % of the wall thickness at the defect's location. The smallest size is found in the casting stub at Location 1, the biggest at Location 7 between the two braces.

A further step of the numerical study consists in the analysis of the SIF values with the aim to generalize and simplify the procedure to determine the allowable initial crack sizes. This simplified procedure should enable an engineer to estimate the allowable initial crack size (and so the defect size) without numerical crack propagation simulations. The SIF results obtained for the typical truss bridge (Figure 6) show that this simplification could be realised by expressing the stress intensity factor $K_I(a)$ in function of a constant correction factor Y:

$$K_I(a) = Y \cdot \sigma_1 \sqrt{\pi \cdot a} \quad (5)$$

$K_I(a)$ stress intensity factor for mode I at crack depth a
Y constant correction factor
σ_1 first principal stress at defect location
a crack depth

The constant correction factor can be obtained by normalising the SIF with the principal stress at Location i. Figure 7 shows the normalised SIF as a function of the square root of the depth $\sqrt{a}$. The constant correction factor value can be extracted from the slope of the regression curve, also shown in the Figure 7.

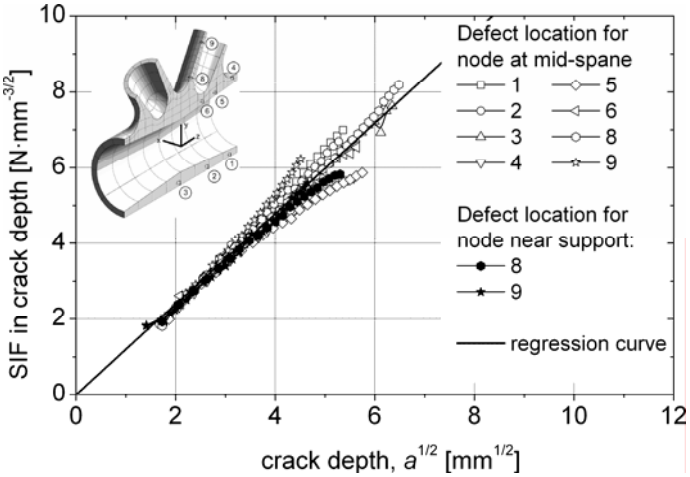

Figure 7. Normalised SIF at different crack locations in nodes at midspan and near the support

Table 2 summarises the values of the constant correction factor in the crack depth (Y_a) and in crack length (Y_c). In general, the correction factor is not constant, but depends for example on the position of the crack in the node and on the crack shape. This simplification shows that it can be assumed constant in cast steel nodes. The factors for an inner crack are nearly equal to 0.64. This is typical for a two dimensional circular inner crack. As seen in Table 2, Y_c is higher than Y_a, indicating that the surface crack propagates faster on the surface than in the depth.

Table 2. Constant correction factor at crack depth and length

	Y_a	Y_c
Surface crack	0.67	0.77
Inner crack	0.62	0.64

An error on the correction factor has a big influence on allowable initial defect size, since the correction factor in Equation (5) is inserted into Equation (4) with an exponent of $m = 3$. Comparison of the allowable initial defect sizes obtained from the numerical SIF and from the constant correction factors shows good agreement (± 20 % deviation) and confirms the validity of the constant correction factor approach.

This allows a simplification of the aforementioned procedure to quantify the initial allowable defect sizes in cast steel nodes used for the typical steel-concrete composite bridge. The simplified steps are summarised in Figure 8:

- Determination of the critical crack size in the case of brittle fracture using the failure assessment diagram with a constant correction factor Y_c to calculate the stress intensity factor $K^c_{I,ULS}(a)$ for ultimate static load.
- Determination of the final crack size as the minimum of 90% of the wall thickness and the critical crack size.
- Back-calculation using the Paris-Erdogan equation with a constant correction factor Y_a to calculate the difference in the stress intensity factor $\Delta K_I(a)$ for the fatigue load.

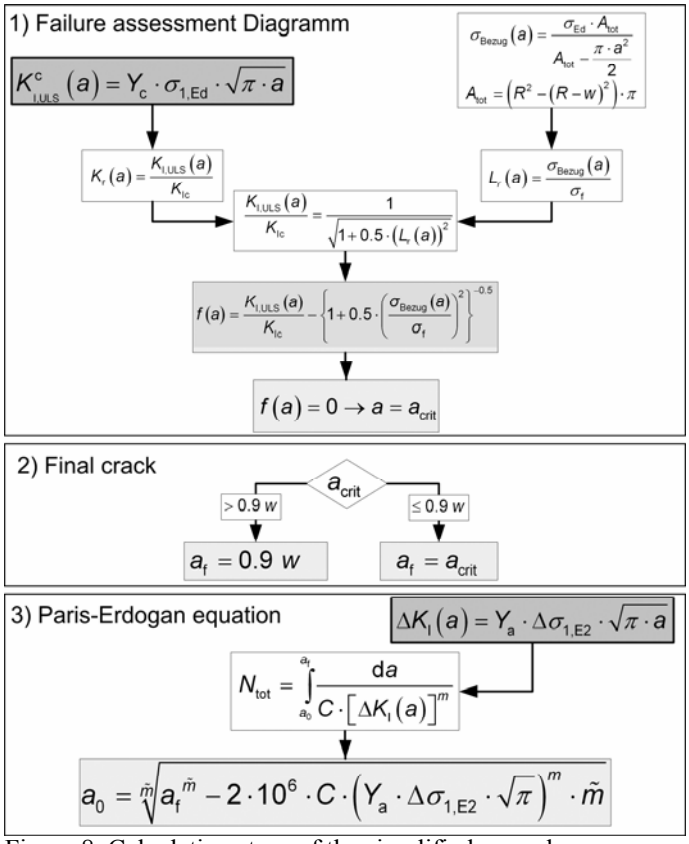

Figure 8. Calculation steps of the simplified procedure

The simplified procedure can now be implemented as an algorithm. This has been done as an user-friendly function for Microsoft Excel® written in Visual Basic for Applications (VBA). With the aid of this algorithm, the allowable initial defect sizes in any cast steel node can be calculated without any crack propagation simulations. The first principal stress under ultimate static and fatigue load at the critical defect location in the cast node is needed as input to the algorithm. The stress can be calculated using a FE or a BE model of the node.

The algorithm was also found suitable for a parametric study in order to determine the influence of the utilisation ratio under ultimate static and fatigue loads, the fracture toughness and the yield strength of the cast steel as well as the node dimensions on the defect size. The algorithm and the results of the parametric study can be found in Haldimann-Sturm (2005).

4 SUMMARY AND CONCLUSIONS

From the interpretation and comparison of the test results between directly welded and cast steel nodes the main points are recalled:

- The welded joints were found to have a fatigue strength of $\Delta\sigma_C = 86$ MPa, which is similar to the fatigue strength of $\Delta\sigma_C = 87$ MPa for the girth butt welds with backing bars.
- The hot spot fatigue strength curve for girth butt welds between casting stubs and CHS members corresponds to $\Delta\sigma_C = 54$ MPa *without* backing bars and $\Delta\sigma_C = 87$ MPa *with* backing bars. When computing the stress range, the stress concentration factor (SCF) due to differences in thickness and diameter of the tubular members and casting stubs must be taken into account.
- A significant difference in the fatigue behavior between welded joints and cast nodes was observed as cracking in the welded joints is directed by high stress concentration at weld toes and in the cast nodes it is caused mainly by weld root defects in the girth butt welds at the casting stubs.
- Cast steel nodes are particularly suited for nodes near or at supports. In the tension chord at midspan, directly welded joints are the better solution regarding fatigue reliability.

From the numerical studies on welded nodes the following recommendations are given:

- The hot-spot stress method has been found to be the only current, widely accepted fatigue design method for welded tubular joints. For the determination of SCFs, existing design guide formulas cannot be extrapolated to low γ values, such as $\gamma \leq 12$, typical to bridges. For these cases, new SCFs were derived from FE analysis. The results show a strong tendency for SCFs to decrease with decreasing γ.
- The recommended minimum SCF at critical joint locations in current design specifications, $SCF = 2.0$, is highly penalizing if applied to welded CHS bridge K-joints. When $\gamma \leq 12$, the recommended minimum SCF can be taken as $SCF = 1.0$ for CHS K-joints.

From the numerical studies on cast steel nodes the following recommendations are given:

- A procedure to quantify the allowable initial casting defect sizes to ensure a balanced design between the various potential crack initiation sites in a cast steel node has been developed for a typical steel-concrete composite bridge. The defect sizes vary between approximately 28 and 88 % of the wall thickness at the location of the casting defect.
- The procedure can be simplified by expressing the SIF with a constant correction factor.

ACKNOWLEDGEMENT

The research carried out is part of the project P591, supervised by the Versuchsanstalt für Stahl, Holz und Steine at the Technische Universität Karlsruhe, which is supported financially and with academic advice by the Forschungsvereinigung Stahlanwendung e. V. (FOSTA), Düsseldorf, within the scope of the Stiftung Stahlanwendungsforschung, Essen. The material presented herein also contains results from previous research sponsored by the Swiss Federal Roads Authority (FEDRO) and the Swiss National Science Foundation (SNF).

REFERENCES

Blair, M., Stevens, T. L., Steel castings handbook, Steel founders' Society of America and ASM International, 1995.

DNV, Fatigue strength analysis of offshore steel structures. Recommended practice RP-C203. Det Norske Veritas, 2001.

Haldimann-Sturm, S.C., Ermüdungsverhalten von Stahlgussknoten in Brücken aus Stahlhohlprofilen, EPFL Thesis No. 3274, Lausanne, 2005.

Marshall, P.W., Design of welded tubular connections, Basis and use of AWS provisions, Elsevier Science Publishers, Amsterdam, 1992.

Milne, I., Ainsworth, R.A., Dowlling, A.R., Stewart, A.T., Assessment of the integrity of structures containing defects, R/H/R6 - Revision 3, Central Electricity Generating Board, Mai 1986.

Raoul, J., Picture taken during construction of the St-Kilian bridge on the A73 highway, near Schleusingen, Germany, 2005.

Schumacher, A., Nussbaumer, A., Experimental study on the fatigue behaviour of welded tubular K-joints for bridges. Engineering Structures, Elsevier Science, 28(5), pp. 745-755.

Schumacher, A. Fatigue behaviour of welded circular hollow section joints in bridges. EPFL Thesis No. 2727, Lausanne, 2003a.

Schumacher, A., Sturm, S., Walbridge, S., Nussbaumer, A., Hirt, M.A. Fatigue design of bridges with welded circular hollow sections ICOM report n^0 489E, ICOM/EPFL, Lausanne, 2003b.

SIA 261, Einwirkungen auf Tragwerke, Schweizerischer Ingenieur- und Architektenverein, 2003.

Sturm, S., Nussbaumer, A., Hirt, M. A., Fatigue behaviour of cast steel nodes in bridge structures, Proceed. of the 10th Int. Symp. on Tubular Structures, pp. 357-364, Tubular Structures X, A.A. Balkema Publishers, Madrid, 2003.

Veselcic, M., Herion, S., Puthli, R., Cast steel in tubular bridges - new applications and technologies, Proceed. of the 10th Int. Symp. on Tubular Structures, pp. 135-142, Tubular Structures X, A.A. Balkema Publishers, Madrid, 2003.

Zhao, X. L.. et al., Design guide for circular and rectangular hollow section joints under fatigue loading, CIDECT, No. 8, TÜV-Verlag Rheinland, Köln, 2000.

Zhao, X. L., Packer, J. A., Fatigue design procedure for welded hollow section joints, Doc. XIII-1804-99, XV-1035-99, IIW, Cambridge, Abington, 2000.